

Fluorescence characteristics of Schiff base-N,N'-bis(salicylidene) trans 1,2-diaminocyclohexane in the presence of bile acid host



Nayan Roy, Pradip C. Paul, T. Sanjoy Singh *

Department of Chemistry, Assam University, Silchar, Assam 788 011, India

ARTICLE INFO

Article history:

Received 8 May 2015

Received in revised form 12 August 2015

Accepted 18 August 2015

Available online xxx

Keywords:

Schiff base

Bile acid

Critical micelle concentration

Binding constant

Fluorescence decay

ABSTRACT

Understanding the formation of bile acid micellar aggregates is of great importance due to its wide biological and pharmacological applications. In this paper, we study the fluorescence properties of Schiff base-N,N'-bis(salicylidene) trans 1,2-diaminocyclohexane (**H₂L**) to understand micelle formation by aggregation of different important bile acids – cholic acid, deoxycholic acid, chenodeoxycholic acid and glycocholic acid by steady state and picosecond time-resolved fluorescence spectroscopy. The fluorescence band intensity was found to increase with concomitant blue shift with gradual addition of different bile acids. Several mean microscopic properties such as critical micelle concentration, polarity parameters and binding constant were estimated in the presence of bile acids. The increase in fluorescence quantum yields, fluorescence decay times and substantial decrease in nonradiative decay rate constants in bile acid micellar environment points to the restricted motion of the fluorophore inside the micellar subdomains.

© 2015 Elsevier B.V. All rights reserved.

1. Introduction

Bile acids (BAs) are steroid acids found predominantly in the bile of mammals which are synthesized from cholesterol in the liver to make up for a small daily loss during the enterohepatic circulation of bile salts. The biosynthesis of bile acid is the principal route of cholesterol consumption in the human body [1]. The one or more α -oriented hydroxyl groups of BAs are put on the concave surface (α -face) of the steroid backbone and the methyl groups are positioned on the opposite convex side (β -face). Free molecules of BAs, normally cylindrical shapes of 20 Å long with a radius of about 3.5 Å, have a great surface activity and inclination to the formation of large aggregates, owing to this difference in orientation of hydrophilic and hydrophobic groups on the steroid ring systems. Prior to secretion by the liver, they are conjugated with either of the amino acids glycine or taurine. Conjugation further increases their water solubility, preventing passive re-absorption once secreted into small intestine. As a result, the concentration of bile acids in small intestine can stay high enough to form micelles and solubilize lipids. Study of formation of micelle of BAs is of great importance for understanding their interaction with biological membranes [2], bile secretion [3], cholesterol solubilization [4] and resveratrol [5] as well as for their roles as promoters for transport of some drugs through the intestine mucous membrane [6].

The formation mechanism and structure of BA micelle as well as the critical micelle concentration (cmc) values were investigated by using

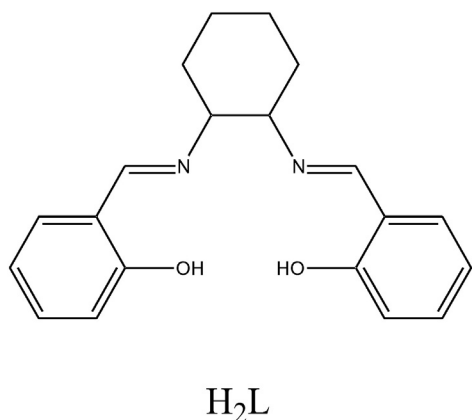
different spectroscopy techniques like NMR, EPR and CD spectroscopy [7–10], X-ray scattering [11], light dispersion and refractometry [12] and also by various physical methods like heat of solution and surface tension measurements [12,13]. In some of the recent publications, Pártay et al. reported molecular dynamics (MD) computer simulation method to study the aggregation process of the sodium salts of cholic acid (CA) and deoxycholic acid (DCA) [14,15]. Such diversity of methods used in the study of BAs further confirms the great importance and existing interest in the study of these biological systems partly because of their uniqueness in the structure when compared with that of the conventional detergent monomers, which has a hydrophilic head group and a long hydrophobic tail and, in part, due to their known importance in biological functions. They are substantially different from synthetic detergents and lipids as shown in regional polarity whereas BAs possess “surface” polarity [16]. The diverse and unique properties pertaining to both chemistry and biology arise from their structural uniqueness. The biological activity of bile acids is mainly based on their surfactant properties in their salt form. They may interact and form mixed micelles with many water insoluble species. Due to different chiral centers present in BAs, their carboxylic and hydroxyl groups can be easily modified for much other application used in construction of artificial receptors and supramolecular architectures. For example, it has recently been reported that the promotory action of BAs in transportation of drugs in biological system depends on their cmc values [17]. So, determination of cmc values of different BA micellar systems is of great importance for elucidating the mechanism of their action. Nichifor et al. studied the aggregation behavior of BA modified dextran using N-phenyl-1-naphthyl amine as a fluorescence probe and reported that the cmc value depends on the nature of hydrophobic moiety and

* Corresponding author.

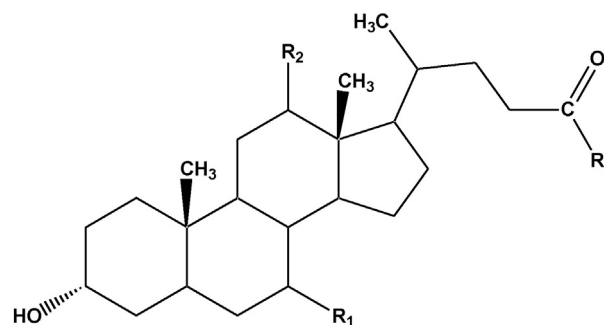
E-mail addresses: takhelsingh@gmail.com, singhsanjoy2002@yahoo.co.in (T. Sanjoy Singh).

the degree of substitution [18]. Fluorescence probes like fluorescein isothiocyanate and also other polycyclic aromatic hydrocarbons having wide range of aqueous solubility were used to determine the cmc value of sodium taurocholate in water [19]. Matsuoka et al. used pyrene as the fluorescence probe to determine the cmc of sodium salt of DCA [20], whereas, Zhang et al. measured the fluorescence anisotropy of 1,6-diphenyl-1,3,5-hexatriene to study the micellization of CA salt [21]. In our earlier paper, we also determine the cmc of different BAs using intramolecular charge transfer (ICT) probe [22]. Such diversity of different methods used to determine the formation mechanism and structure of BAs as well as several mean microscopic properties like cmc, polarity parameters and binding constant indicates its great importance and existing interest in research for further investigations.

Schiff bases named after Hugo Schiff, are the compounds containing azomethine group ($-\text{HC}=\text{N}-$) which play a significant importance in chemistry especially in the development of Schiff base complexes, because they are potentially capable of forming stable complexes with different metal ions [23]. Schiff base leads to synthesis of various bioactive compounds which shows a variety of biological activities including antibacterial, antifungal, anticancer and herbicidal activities [24]. However, fluorescence characteristics of Schiff base in different organized media, which can compartmentalize solvents and solutes as well as sequester them from the bulk environment, are very rare in the literature. So, interest in the binding of Schiff base ligand to different bile acid micellar media has been motivated to prompt the microenvironment of the micellar systems as the fluorescence emission spectra of this Schiff base (H_2L) shows huge fluorescence maxima shift in homogenous buffer solution compared to nonpolar solvent like 1,4-dioxane. The extreme sensitivity of this probe to polarity prompted us to study in a variety of microheterogeneous medium like synthetic detergent where the polarity decreases gradually from the bulk aqueous phase to the hydrocarbon micellar core. Studies based on a completely different class of amphiphilic compounds, like BAs and their salts, as an alternative to the synthetic detergent or cyclodextrins to improve luminescence analysis are scantily observed [25,26]. Hence, the aim of this work is to determine several mean microscopic properties such as cmc, polarity parameters and binding constant by the method of fluorescence spectroscopy. So, in the present work, we report the fluorescence characteristic of H_2L (Scheme I) in presence of different bile acids – cholic acid (CA), deoxycholic acid (DCA), chenodeoxycholic acid (CDCA) and glycocholic acid (GCA) (Scheme II) by steady state and picosecond time-resolved fluorescence spectroscopy. Here, several mean microscopic properties such as critical micelle concentration, polarity parameters and binding constant were estimated in the presence of bile acids and reported in this paper. The increase in fluorescence quantum yields, fluorescence decay times and substantial decrease in nonradiative decay rate constants in bile acid micellar environment points to the restricted motion



Scheme I. Schematic diagram of N,N' -bis(salicylidene) trans 1,2-diaminocyclohexane (H_2L).



Scheme II. General structure of bile acids (BAs) used in this work.

of the fluorophore inside the micellar subdomains. The present work can be extended to understand the aggregation behavior and structure of the microenvironments of different biologically important heterogeneous systems like proteins, lipids and enzymes using H_2L as fluorescent probe.

2. Materials and method

2.1. Materials

N,N' -Bis(salicylidene) trans 1,2-diaminocyclohexane (H_2L) was designed and synthesized by one step condensation of salicylaldehyde and 1,2-diaminocyclohexane in absolute ethanol (Scheme I) and characterized by FT-IR, ^1H and ^{13}C NMR and elemental analysis [27]. CA, DCA, CDCA and GCA were all obtained from Sigma Aldrich Chemical Co. (Product no. C1129, D2510, C9377 and G2878, respectively) and used as received without further purification (Scheme II). The water used as solvent in all the measurements was obtained from Elix10 water purification system (Millipore India Pvt. Ltd.). All experiments were carried out at room temperature (298 K). Bile acids were dissolved in Tris-HCl buffer (pH 9.2). The ligand concentration ($\sim 1.2 \times 10^{-5}$ mol dm^{-3}) was low enough to avoid any aggregation and kept constant during the variation of bile acids concentration.

2.2. Physical measurements

Steady-state absorption spectra were recorded on a Shimadzu UV-1601PC absorption spectrophotometer and fluorescence spectra were obtained in a PerkinElmer LS 45 spectrofluorimeter. Quartz cuvettes of 10 mm optical path length received from Perkin-Elmer, USA (part no. B0831009) and Hellma, Germany (type 111-QS) were used for measuring absorption and fluorescence spectra, respectively. In both fluorescence emission and excitation spectra measurements, 5 nm bandpass was used in the excitation and emission side. The steady state anisotropy (r) can be determined by using the following equation [28]:

$$r = \frac{I_{VV} - GI_{VH}}{I_{VV} + 2GI_{VH}} \quad (1)$$

where I_{VV} is the fluorescence intensity when both the excitation and emission polarizers are oriented vertically and I_{VH} is the fluorescence intensity when the excitation polarizer is vertically and the emission polarizer is horizontally oriented.

G is the correction factor for the sensitivity of the detector to the polarization direction of the emission and is defined as:

$$G = \frac{I_{HV}}{I_{HH}} \quad (2)$$

where I_{HV} is fluorescence intensity with the excitation polarizer horizontally and the emission polarizer vertically oriented, I_{HH} is the

fluorescence intensity with both the excitation and emission polarizers oriented horizontally.

Fluorescence quantum yields (ϕ_f) were calculated by comparing the total fluorescence intensity under the whole fluorescence spectral range with that of a standard ($\phi_f = 0.546$, quinine sulfate in 1 M sulfuric acid [29]) using the following equation.

$$\phi_f^i = \phi_f^s \cdot \frac{F^i}{F^s} \cdot \frac{1 - 10^{-A^s}}{1 - 10^{-A^i}} \cdot \left(\frac{\eta^i}{\eta^s} \right)^2 \quad (3)$$

where F is the total fluorescence intensity under whole fluorescence spectral curve, A^i and A^s are the optical densities of the sample and standard, respectively and η^i is the refractive index of the solvent at 298 K.

The fluorescence decay curves in homogeneous buffer solution of pH 9.2 as well as in the presence of different bile acids – CA, DCA, CDCA and GCA were obtained using LED based time-correlated single photon counting (TCSPC) system obtained from Photon Technology International (PTI). The instrument response function (IRF) was obtained at 340 nm using a dilute colloidal suspension of dried non-dairy coffee whitener. The half width of the IRF was ~ 100 ps. The samples were excited at 340 nm and the fluorescence emission was collected at corresponding emission wavelength. The number of counts in the peak channel was at least 10,000. In fluorescence lifetime measurements, the emission was monitored at the magic angle (54.7°) to eliminate the contribution from the decay of anisotropy.

3. Results and discussion

3.1. Steady state spectral properties

The absorption spectrum of $\mathbf{H}_2\mathbf{L}$ in homogeneous buffer solution of pH 9.2 shows a broad band with the maximum centered at around 320 nm. The fluorescence emission spectrum of $\mathbf{H}_2\mathbf{L}$ appears at 494 nm in homogeneous buffer solution. However, the absorption maxima for the buffer solution of $\mathbf{H}_2\mathbf{L}$ were practically unaffected by the presence of added bile acids. The fluorescence spectral position is strongly dependent on the amount of bile acid in solution. Here, the fluorescence emission maxima of $\mathbf{H}_2\mathbf{L}$ in different BAs micellar media are 422 nm, 410 nm, 425 nm and 419 nm in the case of CA, DCA, CDCA and GCA, respectively and are shown in Fig. 1 and the obtained values are reported in Table 1.

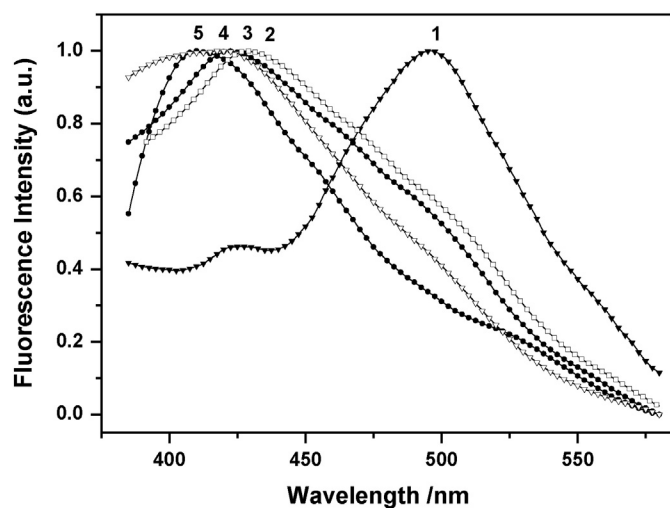


Fig. 1. Fluorescence emission spectra of $\mathbf{H}_2\mathbf{L}$ in buffer solution (1), CDCA (2), CA (3), GCA (4) and DCA (5) ($\lambda_{\text{exc}} = 320$ nm). The concentrations are in mM: (i) 25.9 (CA), (ii) 24.4 (DCA), (iii) 12.6 (CDCA) and (iv) 28.2 (GCA).

Table 1

Fluorescence properties of $\mathbf{H}_2\mathbf{L}$ in homogeneous buffer solution of pH 9.2 and in presence of different bile acids.

Environment	$\lambda_a^{\text{max}}/\text{nm}^a$	$\lambda_f^{\text{max}}/\text{nm}^b$	$\Delta\nu_{\text{fwhm}}/\text{cm}^{-1c}$	$\nu_{0,0}/\text{cm}^{-1d}$	$\Delta\nu_{\text{SS}}/\text{cm}^{-1e}$
Water	325	494	4037	30,172	10,526
CA	322	422	9871	30,518	7359
DCA	328	410	6835	25,524	6097
CDCA	325	425	9239	31,256	7239
GCA	324	419	9531	33,183	6997

^a Absorption maxima.

^b Fluorescence maxima.

^c Fluorescence spectral width at half maximum.

^d Intersection of normalized absorption and fluorescence emission spectra.

^e Stokes shift.

As the fluorescence emission spectrum was strongly dependent on the amount of BAs in solution, gradual addition of CA, DCA, CDCA and GCA is associated with a blue shift in the fluorescence emission maximum along with increase in fluorescence quantum yield (Fig. 2) suggesting that the environment around the probe gets perturbed in the presence of different bile acids. In analogy with the results discussed previously for $\mathbf{H}_2\mathbf{L}$ spectral properties in the presence of different micellar solutions, a blue shift of the fluorescence emission maximum suggests that the polarity of the micellar environment is less than the polarity of the bulk water. While the fluorescence spectral blue shift for $\mathbf{H}_2\mathbf{L}$ is about 6097 cm^{-1} in DCA compared to its position in homogeneous buffer solution, in CA, CDCA and GCA the shifts are 7359 cm^{-1} , 7239 cm^{-1} and 6997 cm^{-1} , respectively. This indicates that the micropolarity around the probe in these BAs is similar and appreciably different from that in DCA. Apart from the shift in spectral position, fluorescence intensity of $\mathbf{H}_2\mathbf{L}$ increases remarkably in the presence of all the bile acid. This observation is true for all the bile acid studied here and can be rationalized on the basis of the binding of the probe in a less polar site within the micellar aggregates as compared to bulk aqueous phase.

The changes of the emission profile of $\mathbf{H}_2\mathbf{L}$ with gradual addition of different bile acids – CA, DCA, CDCA and GCA suggest its movement from bulk aqueous phase to micellar environment. To understand the rigidity of the microenvironment, the steady state fluorescence anisotropy measurements were carried out which provide important information regarding the binding and location of the probe molecule in bile acids aggregated systems. The steady state anisotropy of $\mathbf{H}_2\mathbf{L}$ in the presence of different BA systems is 0.17, 0.21, 0.14 and 0.19 respectively for CA, DCA, CDCA and GCA. These fluorescence anisotropy values are comparatively very high compared to free ligand (0.02). This observation clearly indicates that the probe molecule strongly interact with different bile acids upon incorporation into the different binding sites. The increase in anisotropy value suggests that the probe molecule must feel restriction of its rotational motion on moving from the bulk aqueous phase to micellar environment [30].

3.2. Determination of critical micelle concentration

The change in fluorescence emission maximum and intensity with gradual addition of BAs (Fig. 2), can be attributed to the passage of the probe ($\mathbf{H}_2\mathbf{L}$) molecule from a highly polar aqueous phase to a relatively nonpolar micellar phase. Surfactant molecules form aggregates at cmc under certain environmental conditions and hence, the microenvironment below and above critical micelle concentration are quite distinct. At lower surfactant concentration, the change in fluorescence response is not very prominent. However, after a certain micellar concentration, both fluorescence emission position and intensity show a drastic change. These sharp break points are conventionally assigned to critical micelle concentration. Here, $\mathbf{H}_2\mathbf{L}$ has been used to estimate the cmc values for different bile acids – CA, DCA, CDCA and GCA. The cmc values

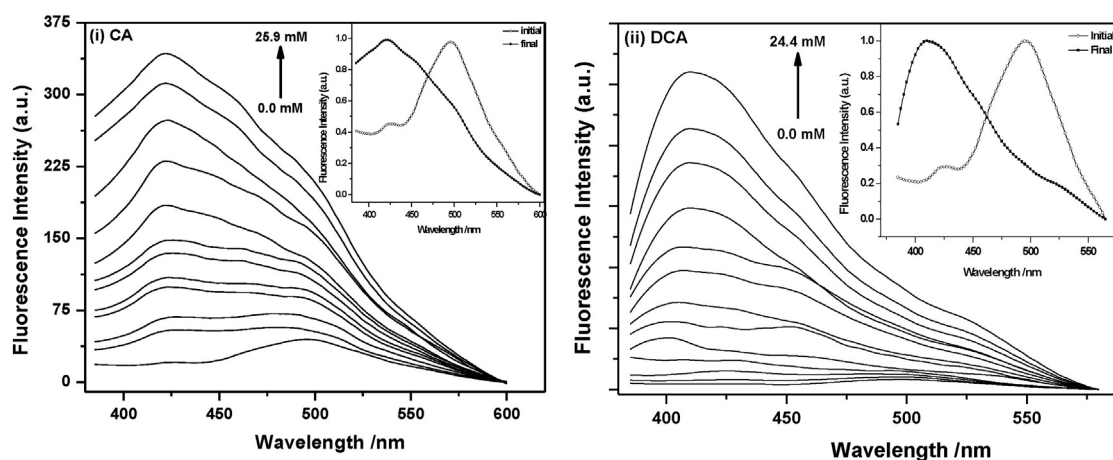


Fig. 2. Variation of H₂L fluorescence spectra with increasing concentration of CA (i) and DCA (ii) ($\lambda_{\text{exc}} = 320$ nm). The concentration of bile acids is in mM: [CA] = 0.0, 1.4, 2.8, 4.2, 6.4, 8.9, 10.6, 12.3, 14.9, 17.9, 21.9 and 25.9 and [DCA] = 0.0, 1.8, 2.8, 4.2, 5.6, 7.6, 8.4, 9.8, 12.5, 17.3, 21.2 and 24.4. Inset shows the spectra in the presence and absence of bile acids.

were estimated from the maximum of the derivative plot of fluorescence intensity with BA concentration (Fig. 3) and the estimated cmc values are 8.7 mM, 5.6 mM, 8.8 mM and 11.2 mM respectively for CA, DCA, CDCA and GCA. These values were also reported in Table 2. As can be seen from Table 2, the estimated cmc values obtained for different BAs from experimental data are in good agreement with the literature values obtained through other methods [31,32]. The close agreement in the measured microscopic properties of micellar systems in this study with the literature reported values obtained by using entirely different type of probe indicates the insensitivity of the probe molecule in these measurements.

The striking feature of BA aggregation scheme is that it is characterized by at least two cmc values. According to the primary–secondary micelle model of Small [33], at low concentrations, the BAs form small primary micelles with a characteristic cmc value. In this micelle, the BAs turn toward each other by their hydrophobic β -face. At the concentration range beyond second cmc, these primary micelles attach together to form large secondary micelles by hydrogen bonding interactions through their hydrophilic outer surface. It is to be noted that the concentration range of BAs, used in the present study, is limited to monitor the formation of the primary micelles only.

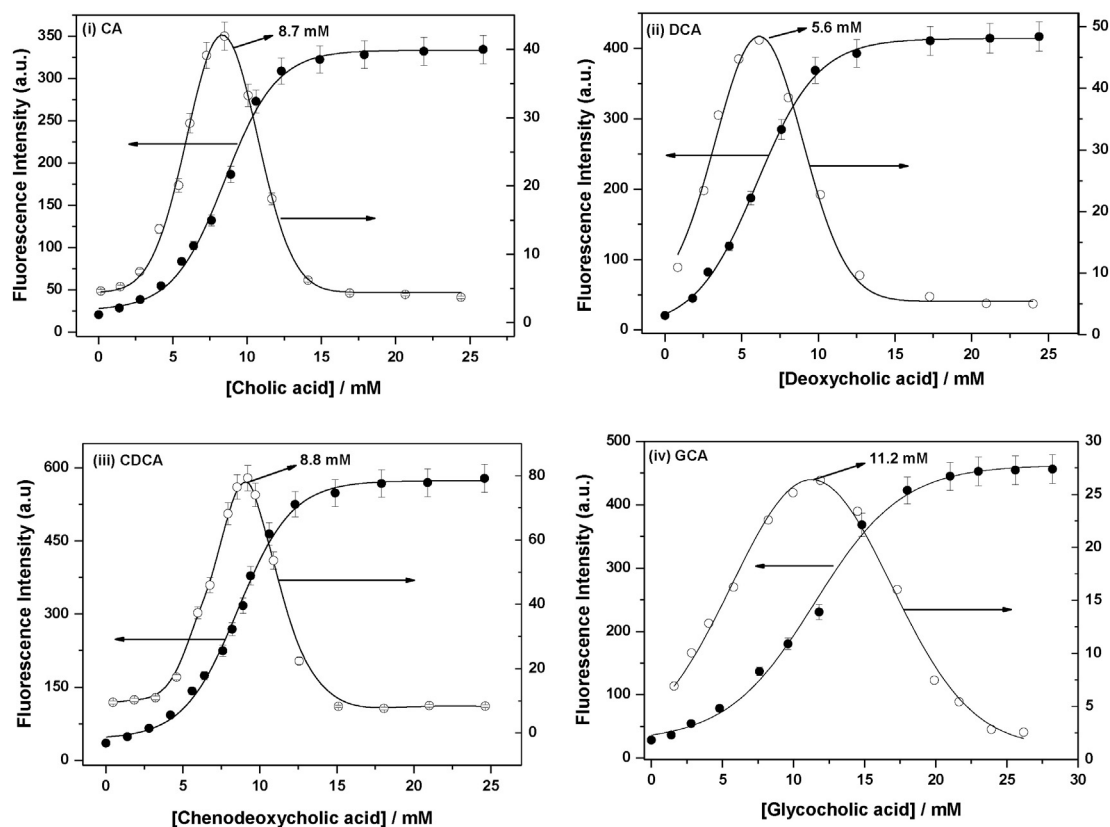


Fig. 3. Variation of H₂L fluorescence intensity with different bile acids at specific wavelength for (i) CA, (ii) DCA, (iii) CDCA and (iv) GCA, respectively. Solid line with open circles (right axis) represents spline fit of the derivative data in (i) CA, (ii) DCA, (iii) CDCA and (iv) GCA; the maximum of which indicates cmc for the micelization process.

Table 2

Critical micelle concentration (cmc), dielectric constant (ϵ) and $E_T(30)$ parameters as well as binding constant (K_S) obtained for different bile acids using H_2L as a fluorescence probe at pH 9.2.

Properties	Estimated values			
	CA	DCA	CDCA	GCA
cmc/mM ^a	8.7	5.6	8.8	11.2
[literature value]	[6.5–9.5]	[4.7]	[9.0]	[12.0]
Dielectric constant ^b (ϵ)				
(i)	40.6	23.6	39.0	35.7
(ii)	15.4	1.94	18.6	12.1
$E_T(30)$ parameters ^c				
(i)	48.7	42.8	48.1	47.0
(ii)	36.9	31.7	38.4	35.8
$K_S^d, /10^2, M^{-1}$	0.72	1.25	0.68	0.78
(\pm error)	(0.01)	(0.02)	(0.02)	(0.01)

^a Estimated from the derivative plot of fluorescence intensity variation with bile acid concentration.

^b Obtained from linear plots of (i) Stokes shift ($\Delta\nu_{ss}$) and (ii) fluorescence maxima (ν_f) vs. ϵ .

^c Obtained from linear plots of (i) Stokes shift ($\Delta\nu_{ss}$) and (ii) fluorescence maxima (ν_f) vs. $E_T(30)$.

^d Estimated from the slope of linear relation given in Eq. (14).

3.3. Polarity parameters

Difference in fluorescence properties of the probe in bile acid micellar environment with those of the homogeneous solvents helps us to estimate the polarity of the microenvironment indicating the location of the probe which is of great importance in the biological systems. However, it should be kept in mind that the polarity of different heterogeneous media is huge different from those of homogeneous medium. Attention has been drawn to estimate the empirical polarity scale, $E_T(30)$ using the following set of equations:

$$\nu_f (\text{cm}^{-1}) = (28417.1 \pm 264.3) - (127.9 \pm 6.5) \times E_T(30) \quad (4)$$

$$\Delta\nu_{ss} (\text{cm}^{-1}) = (-3136.2 \pm 245.5) + (215.5 \pm 6.1) \times E_T(30) \quad (5)$$

where, fluorescence energy and Stokes shift are represented by ν_f and $\Delta\nu_{ss}$, respectively. Similarly, dielectric constant (ϵ) for different BA systems was also evaluated using the following set of equations:

$$\nu_f (\text{cm}^{-1}) = (24490.3 \pm 225) - (51.6 \pm 5.7) \times \epsilon \quad (6)$$

$$\Delta\nu_{ss} (\text{cm}^{-1}) = (4337.5 \pm 301.3) + (74.4 \pm 8.3) \times \epsilon. \quad (7)$$

The estimated polarity parameters of H_2L in different BA system are reported in Table 2 and the corresponding plots are shown in Fig. 4. To be best of our knowledge, there is no literature data available for the interior polarity of BAs or their salts; so it was not possible to make any direct comparison of the estimated parameters. However, in one of the relatively recent report by Lee et al. [34], it was shown that the interior polarity of the microaggregates formed from DCA modified chitosan is substantially reduced when compared with bulk water. Similarly, in our earlier paper [22], we also observed a decrease in polarity of the BA systems when compared with bulk water phase. From Table 2, it is shown clearly that the polarity of the microenvironment is in the order of CDCA > CA > GCA > DCA which indicate more nonpolar environment in DCA compared to other BA systems, as also evidenced from the fluorescence emission maxima obtained as described earlier.

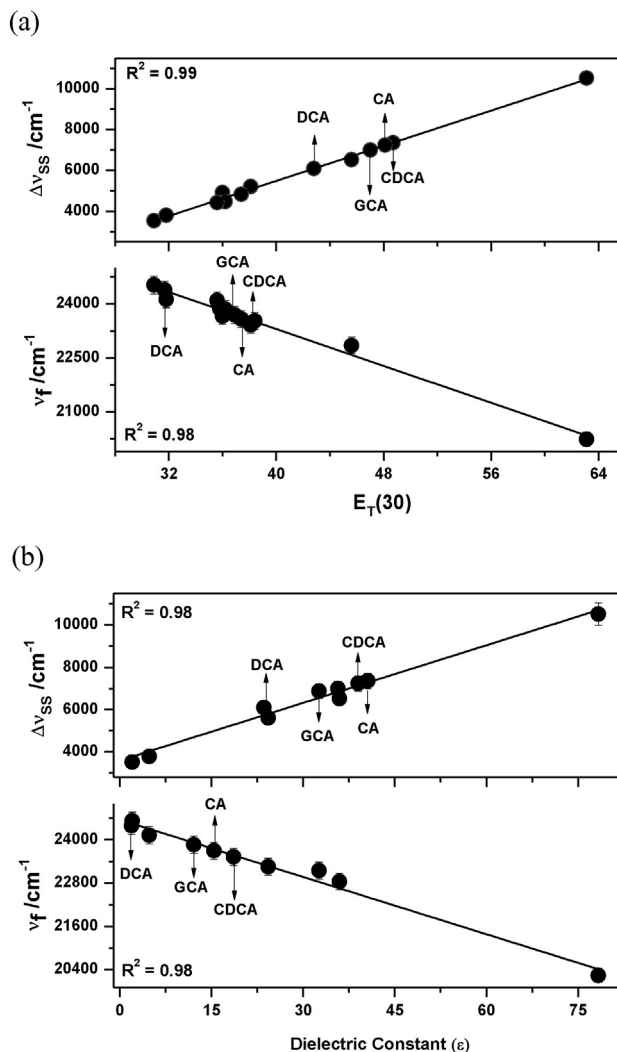


Fig. 4. Plots of fluorescence emission energy (ν_f) and Stoke's shift ($\Delta\nu_{ss}$) against (a) $E_T(30)$ parameter and (b) dielectric constants (ϵ) of H_2L .

3.4. Estimation of the probe-micelle binding constant

The binding of a probe to micelles can be described by the following equilibrium [35]:



where, S_a and S_m denote the substrate concentrations expressed as molarities in terms of total volume of solution in aqueous phase and in micellar pseudophase.

The equilibrium constant for the process (Eq. (8)), often termed as binding constant, is given by

$$K_S = \frac{[S_m]}{[S_a][D_m]} \quad (9)$$

It is known that for the formation of primary micelle in BAs, the aggregation number is very small and it shows rather weak dependence on the surfactant concentration between the two cmc values. However, in the vicinity of higher cmc value, the aggregation number increases very sharply. For example, the mean aggregation number of the sodium salt of both CA and DCA is about 2–5 within the concentration range of 50 mM; however, it changes abruptly to about 20 at ~100 mM surfactant concentration [36].

The maximum surfactant concentration, for all the BAs used in this study, is always within 30 mM range and the aggregation number for the primary micelle formation can be assumed to be constant. With this approximation, the total substrate concentration (S_t) and total detergent concentration (D_t) can be written as $[S_a] + [S_m]$ and $[S_m] + [D_m] + \text{cmc}$, respectively.

The fraction of micellar associated substrate is defined as

$$f = \frac{[S_m]}{[S_t]} \quad (10)$$

Then from Eq. (9), one obtains

$$\frac{f}{1-f} = K_S \{ [D_t] - [S_t] \times f \} - K_S \times \text{cmc} \quad (11)$$

Under the condition of $[S_m] \ll [D_t]$ and $[D_t] \gg \text{cmc}$, the above equation can be approximated as

$$\frac{f}{1-f} = K_S \times [D_t] \quad (12)$$

Experimentally, f can be calculated by steady state fluorescence experiments in the presence and absence of micellar systems as follows:

$$f = \frac{F - F_0}{F_m - F_0} \quad (13)$$

where, F , F_0 and F_m are the area under the whole fluorescence emission spectra of the probe in surfactant, water and in fully micellized condition, respectively. Substituting the value of f in Eq. (12), one can write

$$\frac{F - F_0}{F_m - F} = K_S \times [D_t] \quad (14)$$

A plot of $(F - F_0) / (F_m - F)$ vs $[D_t]$ gives a straight line, the slope of which gives the value of the binding constant, K_S . The binding constant value of $\mathbf{H}_2\mathbf{L}$ with different BA systems are $0.72 \times 10^2 \text{ M}^{-1}$, $1.25 \times 10^2 \text{ M}^{-1}$, $0.68 \times 10^2 \text{ M}^{-1}$ and $0.78 \times 10^2 \text{ M}^{-1}$ respectively for CA, DCA, CDCA and GCA. These values were also reported in Table 2 and some of the representation plots are shown in Fig. 5. Interestingly, the binding constant of $\mathbf{H}_2\mathbf{L}$ with different BA systems are in the order of $\text{DCA} > \text{GCA} > \text{CA} > \text{CDCA}$ indicating a more nonpolar environment of the probe in DCA compared to other BA systems, as also evidenced from the fluorescence emission maxima obtained as described earlier.

3.5. Time-resolved fluorescence measurements

Fluorescence lifetime of a fluorophore in a micellar solution serves as a sensitive parameter for exploring the local environment around the fluorophore. It also contributes to the understanding of different

interactions between the probe and the micelle [37,38]. On the basis of this, time-resolved fluorescence studies were performed on $\mathbf{H}_2\mathbf{L}$ under pre-micellar as well as fully primary micellized state in all different bile acids and also in homogeneous buffer medium and the findings are reported in Table 3. The homogeneous buffer solution of $\mathbf{H}_2\mathbf{L}$ fit very well with single exponential decay. However, in micellar solutions, the decay curves show contributions from more than one component. The fluorescence decay curves were analyzed by non-linear least-square iterative convolution method using Eq. (15) based on Lavenberg–Marquardt [39] chi-square (χ^2) minimization algorithm (Eq. (16))

$$F(t) = \sum_i a_i \exp(-t/t_i) \quad (15)$$

α_i is the associated pre-exponential factor corresponding to the decay time τ_i .

$$\chi^2 = \frac{\sum_{i=1}^N [y_i - f(x_i)]^2}{N - P} \quad (16)$$

N is the number of data points and P is the number of free parameters in the fitting function. The reliability of fitting was checked by numerical value of reduced chi-square (χ^2) and also Durbin–Watson (DW) parameter.

It is to be noted that in fully primary micellized condition, a three exponential function was needed to fit the experimental data as demonstrated by visual inspection of the distribution of weighted residuals with time (Fig. 6). However, as it is seen from Table 3 that the amplitude of the short nanosecond component is larger compared to long nanosecond component in all different BAs. Multiexponential decay of fluorescence is quite common and it is often difficult to mechanistically assign the various components of the decay. The fluorescence lifetime values of the probe in different BA micelles are clearly more than those in homogeneous buffer solution. Even if we assume that the diffusion of the probe molecule is rather slow in micellar medium, there is always a probability that the probe molecule in different microdomains of BA micelles are excited simultaneously to give multiexponential fluorescence decay. Instead of giving too much importance to individual decay components, we define the mean fluorescence decay time of the fluorophore inside different BA micelles using Eq. (17) to discuss the fluorescence decay behavior.

$$\langle \tau \rangle = \sum_i a_i \times \tau_i \quad (17)$$

The calculated mean fluorescence decay values are 2.18 ns, 4.68 ns, 4.23 ns, 4.77 ns and 6.16 ns for buffer, CA, DCA, CDCA and GCA respectively. These values were also listed in Table 3. It is interesting to note that the mean fluorescence decay time in BAs micellar media are

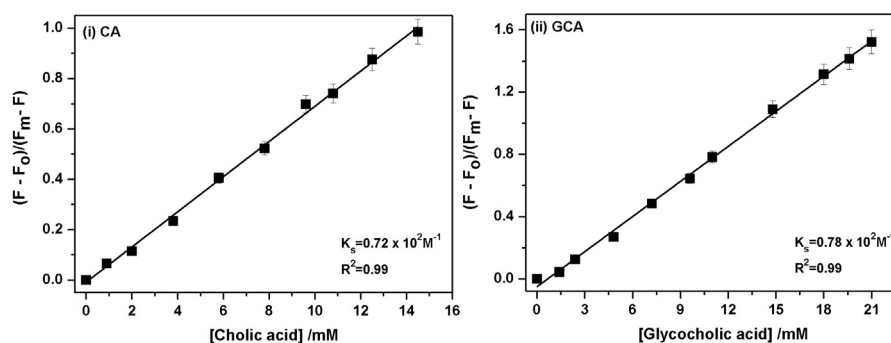


Fig. 5. Variation of $(F - F_0) / (F_m - F)$ with total bile acids concentration $[D_t]$ for CA (i) and GCA (ii). The binding constant value, K_S was calculated from the slope of the linear relation using Eq. (14).

Table 3
Fluorescence quantum yield (ϕ), decay time (τ), mean fluorescence decay time ($\langle\tau\rangle$), radiative (κ^r) and total nonradiative (κ^{nr}) decay constants of H_2L in homogeneous buffer solution as well as in presence of different bile acids.

Medium	$\phi/10^{-3}$	Fluorescence decay time (τ)			$\langle\tau\rangle$ ns	κ^r $/10^7 \text{ s}^{-1}$	κ^{nr} $/10^9 \text{ s}^{-1}$
		$\tau_1/\text{ns}(\alpha_1)$	$\tau_2/\text{ns}(\alpha_2)$	$\tau_3/\text{ns}(\alpha_3)$			
Buffer	3.4	2.18(1.0)	–	–	2.18	0.15	0.46
CA	28.5	1.63(0.48)	5.04(0.38)	14.2(0.14)	4.68	0.61	0.21
DCA	40.6	1.34(0.54)	4.96(0.34)	15.2(0.12)	4.23	0.96	0.23
CDCA	32.4	1.48(0.52)	5.84(0.36)	15.8(0.12)	4.77	0.68	0.20
GCA	36.5	2.11(0.57)	6.74(0.32)	25.5(0.11)	6.16	0.59	0.16

about 2–3 times larger than the corresponding values in homogeneous buffer solution. Fluorescence quantum yield (ϕ) calculated from the area of the total fluorescence emission over the whole spectral range, the radiative (κ^r) and nonradiative (κ^{nr}) decay rate constants calculated from Eq. (18) are also listed in Table 3. The increase in fluorescence quantum yields (ϕ), fluorescence decay times and substantial decrease in nonradiative (κ^{nr}) decay rate constants in BAs micellar environment points to the restricted motion of the fluorophore inside the micellar subdomains. From Table 3, the fluorescence decay times increases in the order of GCA > CDCA > CA > DCA and nonradiative decay rate constants as DCA > CA > CDCA > GCA in BAs micellar environment which indicates the restricted low-frequency motion of the fluorophore inside the micellar subdomains as discussed earlier.

$$\kappa^r = \phi/\langle\tau\rangle; \kappa^{nr} = (1-\phi)/\langle\tau\rangle \quad (18)$$

3.6. Comparison with binding of the probe in synthetic detergents

Although, the spectroscopic properties of H_2L in the presence of BAs show similar trend like blue shift with increase in fluorescence emission intensity as in synthetic detergents, some of the calculated parameters

show marked differences in these environments. For example, the shift in fluorescence maximum of H_2L under fully micellized condition of BA is about 6097 cm^{-1} from that in homogeneous buffer solution. However, in case of synthetic detergents, the maximum shift was observed in case of triton X-100 (TX-100); which is of the order of 7016 cm^{-1} . These differences can be approximated due to the difference in micellar structure for BAs when compared with synthetic detergents. In contrast to the spherical nature of the pseudo-particle formed due to the self aggregation of linear surfactant molecules like SDS, CTAB and TX-100, the BAs consist of a rigid steroid backbone giving rise to the concave side with polar hydroxyl group (α -face) and the methyl groups in the convex side (β -face). Aggregation of BAs in aqueous solution is due to hydrophobic interaction of the apolar β -faces of steroid backbones with possibility of further aggregation through hydrogen bonding in the α -faces. This unique arrangement based on facial amphiphilicity renders a different aggregation pattern in BAs unlike the conventional surfactants; where, the micellar structure is mostly approximated to be spherical, originated from the mutual arrangement of the head and tail groups with different hydrophobicity [40,41].

Again, the binding constant of H_2L in the presence of BAs is comparatively very low compared to synthetic detergents like SDS, CTAB and TX-100 as reported in Table 2. Here in case of synthetic detergents,

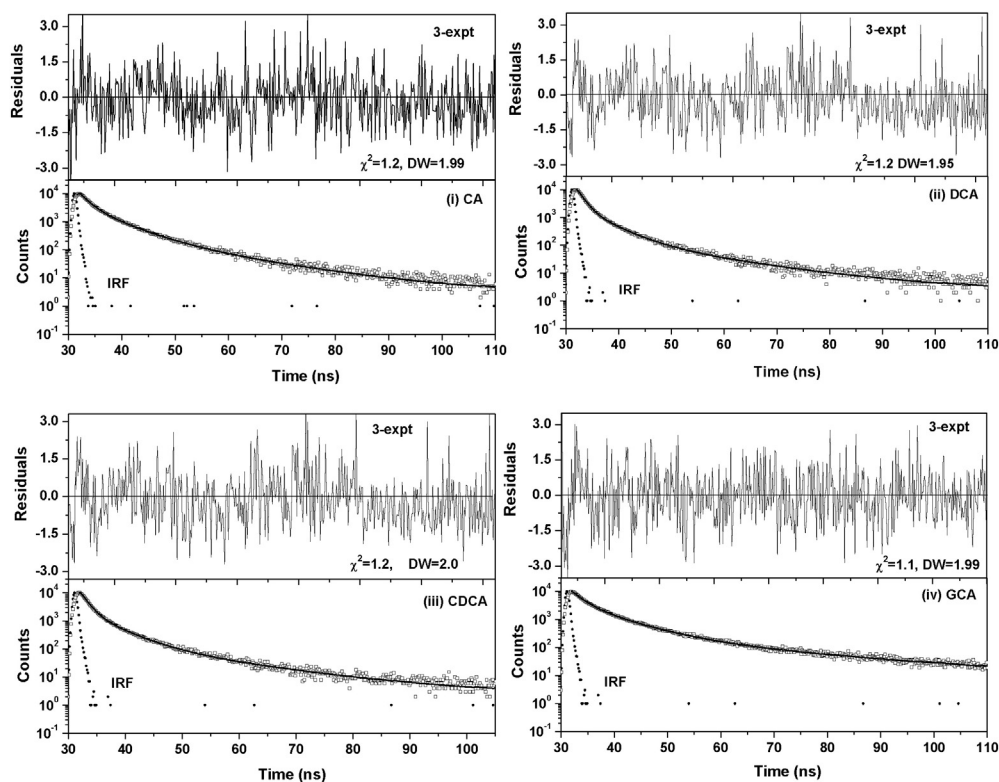


Fig. 6. Time-resolved fluorescence decay profile of H_2L in the presence of different bile acids: CA (i), DCA (ii), CDCA (iii), and GCA (iv), respectively. IRF indicates instrument response function. The upper panels show the distribution of weighted residuals for three exponential fitting along with reduced chi-square (χ^2) and Durbin-Watson (DW) parameters in each case.

the binding constant value of **H₂L** with different detergent systems are $7.2 \times 10^2 \text{ M}^{-1}$, $7.8 \times 10^2 \text{ M}^{-1}$ and $9.6 \times 10^2 \text{ M}^{-1}$ for SDS, CTAB and TX-100 respectively. The difference of fluorescence parameters of **H₂L** in BAs host compared with synthetic detergents is believed to be due to difference in the micellar structure.

4. Conclusions

In this work, we have investigated the fluorescence properties of *N,N'*-bis(salicylidene) trans 1,2-diaminocyclohexane (**H₂L**) inside the micellar environment and is found to be different in bile acid micellar media when compared with homogeneous buffer solution. The blue shift in fluorescence emission maxima, with considerable increase in fluorescence band intensity as well as fluorescence lifetime value indicates the binding of the probe inside the micellar subdomains. Critical micelle concentration obtained by using **H₂L** as a probe in the presence of different bile acids is in good agreement with literature reported values. The fluorescence emission peak position, polarity parameters and binding constant values indicate more nonpolar behavior in DCA compared to others bile acids. However, the difference of fluorescence parameters of **H₂L** in bile acid hosts compared with synthetic detergents is believed to be due to difference in the micellar structure. The present work can be extended to understand the aggregation behavior and structure of the microenvironments of different biologically important heterogeneous systems like proteins, lipids and enzymes using **H₂L** as fluorescent probe.

Acknowledgments

Financial support through UGC-BSR Research Start-Up-Grant project No. F.20-1/2012 (BSR)/20-1(2)(2012)(BSR) from the University Grants Commission (UGC) and Start-Up Research Grant (Chemical Sciences) project No. SB/FT/CS-064/2012 from the Science and Engineering Research Board (SERB), Government of India was gratefully acknowledged by Dr. T. Sanjoy Singh. The authors are indebted to Dr. S. Mitra and his research scholars for their help in TCSPC measurements.

References

- [1] M. Dumont, S. Erlinger, S. Uchman, *Gastroenterology* 79 (1980) 82–89.
- [2] A. Helenius, K. Simons, *Biochim. Biophys. Acta* 415 (1975) 29–79.
- [3] E.R. O'Maille, *J. Physiol.* 302 (1980) 107–120.
- [4] K.H. Kwan, W.I. Higuchi, A.F. Hofmann, *J. Pharm. Sci.* 67 (1978) 1171–1174.
- [5] M. Atanacković, M. Poša, H. Heinle, L. Gojković-Bukarica, J. Cvejić, *Colloids Surf. B: Biointerfaces* 72 (2009) 148–154.
- [6] C.L. Blowe, L. Mokhtarzadeh, P. Venkatesan, S. Babu, H.R. Axelrod, M.J. Sofia, R. Kakarla, T.Y. Chan, J.S. Kim, H.J. Lee, G.L. Amidon, S.Y. Choe, S. Walker, D. Kahne, *Proc. Natl. Acad. Sci. U. S. A.* 94 (1997) 12218–12223.
- [7] D.M. Small, S.A. Penkett, D. Chapman, *Biochem. Biophys. Acta* 176 (1969) 178–189.
- [8] E. Giglio, S. Loreti, N.V. Pavel, *J. Phys. Chem.* 92 (1988) 2858–2862.
- [9] G. Esposito, E. Giglio, N.V. Pavel, A. Zonobi, *J. Phys. Chem.* 91 (1987) 356–362.
- [10] S. Gouin, X. Zhu, *Langmuir* 14 (1998) 4025–4029.
- [11] T. Waernheim, E. Sjoebloom, U. Henriksson, P. Stilbs, *J. Phys. Chem.* 88 (1984) 5420–5425.
- [12] J.P. Kratochvil, H.T. Dellicolli, *Can. J. Biochem.* 46 (1968) 945–952.
- [13] L. Benzamin, *J. Phys. Chem.* 68 (1964) 3575–3581.
- [14] L.B. Pártay, P. Jedlovsky, M. Sega, *J. Phys. Chem. B* 111 (2007) 9886–9896.
- [15] L.B. Pártay, P. Jedlovsky, M. Sega, *Progr. Colloid Polym. Sci.* 135 (2008) 181–187.
- [16] R.N. Redinger, D.M. Small, *Arch. Intern. Med.* 1972 (130) (1972) 618–630.
- [17] M. Poša, S. Kevrešan, M. Mikov, V. Ćirin-Novta, K. Kuhajda, *Eur. J. Drug Metab. Pharmacokinet.* 32 (2007) 109–117.
- [18] M. Nichifor, A. Lopes, A. Carпов, E. Melo, *Macromolecules* 32 (1999) 7078–7085.
- [19] S.M. Meyerhoffer, L.B. McGown, *Langmuir* 6 (1990) 187–191.
- [20] K. Matsuoka, Y. Moroi, *Biochim. Biophys. Acta* 1580 (2002) 189–199.
- [21] X. Zhang, J.K. Jackson, H.M. Burt, *J. Biochem. Biophys. Methods* 31 (1996) 145–150.
- [22] T.S. Singh, S. Mitra, *J. Photochem. Photobiol. B* 96 (2009) 295–305.
- [23] P. Souza, J.A. Garcia-Vazquez, J.R. Masaguer, *Trans. Met. Chem.* 10 (1985) 410–412.
- [24] L.Z. Flores-Lopez, M. Parra-Hake, R. Somanathan, P.J. Walsh, *Organometallics* 19 (2000) 2153–2160.
- [25] K. Bhattacharyya, *Organized Assemblies Probed by Fluorescence Spectroscopy, Reviews in Fluorescence – 2005*, in: C.D. Geddes, J.R. Lackowicz (Eds.), Springer, US 2005, pp. 1–23.
- [26] U. Subudhi, A.K. Mishra, *J. Chem. Sci.* 119 (2007) 169–174.
- [27] N. Roy, H.A.R. Pramanik, P.C. Paul, T.S. Singh, *J. Fluoresc.* 24 (2014) 1099–1106.
- [28] J.R. Lakowicz, *Principle of Fluorescence Spectroscopy*, Plenum, New York, 2006.
- [29] J.N. Demas, G.A. Crosby, *J. Phys. Chem.* 75 (1971) 991–1024.
- [30] D. Chakrabarty, P. Hazra, N. Sarkar, *J. Phys. Chem. A* 107 (2003) 5887–5893.
- [31] B.R. Simonović, M. Momirović, *Mikrochim. Acta* 127 (1997) 101–104.
- [32] B. Natalini, R. Sardella, E. Camaioni, A. Gioiello, R. Pellicciari, *Anal. Bioanal. Chem.* 388 (2007) 1681–1688.
- [33] D.M. Small, *The physical chemistry of cholanic acids*, in: P.P. Nair, D. Kritchevsky (Eds.), *The Bile Acids: Chemistry, Physiology and Metabolism*, vol. 1, Plenum Press, New York, 1971 (ch 8).
- [34] K.Y. Lee, W.H. Jo, I.C. Kwon, Y.-H. Kim, S.Y. Jeong, *Macromolecules* 31 (1998) 378–383.
- [35] C. Hirose, L. Sepulveda, *J. Phys. Chem.* 85 (1981) 3689–3694.
- [36] K. Fontell, *The micellar structure of bile salt solutions*, in: P. Ekwall, K. Groth, V. Runnström-reio (Eds.), *Surface Chemistry*, Munksgaard-Copenhagen 1965, pp. 252–267.
- [37] K.D. Ashby, K. Das, J.W. Petrich, *Anal. Chem.* 69 (1997) 1925–1930.
- [38] A. Maciejewski, J. Kubicki, K. Dobek, *J. Phys. Chem. B* 107 (2003) 13986–13999.
- [39] P.R. Bevington, *Data Reduction and Error Analysis for the Physical Sciences*, McGraw-Hill, Inc, New York, 1969.
- [40] S. Mukhopadhyay, U. Maitra, *Curr. Sci.* 87 (2004) 1666–1683.
- [41] V. De Giorgio, M. Conti (Eds.), *Physics of Amphiphiles, Micelles, Vesicles and Microemulsions*, North-Holland, Amsterdam, 1985.

Glossary of acronyms

H₂L: *N,N'*-bis(salicylidene) trans 1,2-diaminocyclohexane
BAs: bile acids
MD: molecular dynamics
CA: cholic acid
DCA: deoxycholic acid
CDCA: chenodeoxycholic acid
GCA: glycocholic acid
ICT: intramolecular charge transfer
SDS: sodium dodecyl sulfate
CTAB: cetyl trimethyl ammonium bromide
TX-100: Triton X-100
TCSPC: time-correlated single photon counting
PTI: photon technology international
IRF: instrument response function
cmc: critical micelle concentration
DW: Durbin–Watson

Glossary of mathematical terms

$\Delta\nu_{ss}$: Stokes' shift
 ν_f : fluorescence energy
 ϕ_f : quantum yield
 η : refractive index
 K_b : binding constant
 τ_f : fluorescence lifetime
 χ^2 : reduced chi-square
 k^r : radiative decay rate constant
 k^{nr} : nonradiative decay rate constant